```
                                                                                                   Section 1
                          (1) 1          10         20         30         40         50         60             76
     GIPR_human_NP_000155.gp (1) MTTSPILQLLLRLSLCGLLLQRAETGSKG-QTAGELYQRWERYRRECQETLAAAEPPSGLACNGSFDMYVCWDYAA
GIPR_mouse_NP_001074284.gp (1) ---MPLRLLLLLWLWG--LQWAETDSEGQTTTGELYQRWEHYGQECQKMLETTEPPSGLACNGSFDMYACWNYTA
       GIPR_rat_NP_036846.gp (1) ---MPLRLLLLLWLWGLSLQRAETDSEG-QTTGELYQRWERYGWECQNTLEATEPPSGLACNGSFDMYACWNYTA
                                                                                                   Section 2
                         (77) 77          90         100        110        120        130        140          152
     GIPR_human_NP_000155.gp (76) PNATARASCPWYLPWHHHVAAGFVLRQCGSDGQWGLWRDHTQCENPEKNEAFLDQRLILERLQVMYTVGYSLSLAT
GIPR_mouse_NP_001074284.gp (72) ANTTARVSCPWYLPWFRQVSAGFVFRQCGSDGQWGSWRDHTQCENPEKNGAFQDQTLILERLQIMYTVGYSLSLTT
       GIPR_rat_NP_036846.gp (73) ANTTARVSCPWYLPWYRQVAAGFVFRQCGSDGQWGSWRDHTQCENPEKNGAFQDQKLILERLQVVYTVGYSLSLAT
```

Supplement 1: GIPR-N terminal extracellular domain sequences.
Shown are the human, mouse and rat extracellular domain amino acids (22-139) that were used to generate recombinant rabbit (for biophysical analyses) or human (as antigen for immunization) Fc fusion proteins respectively.

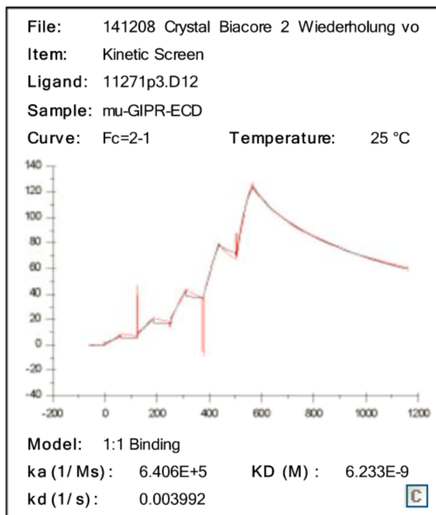

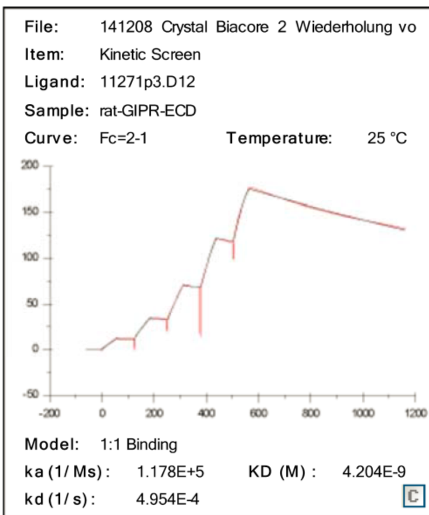

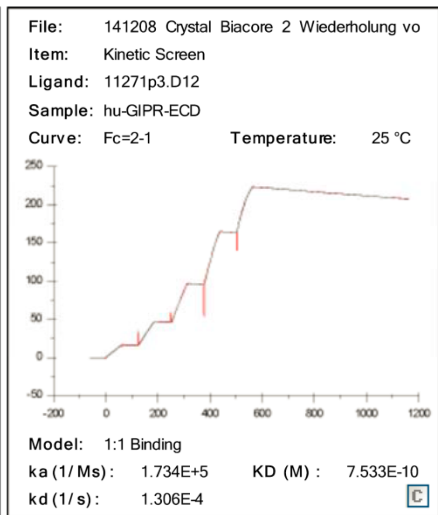

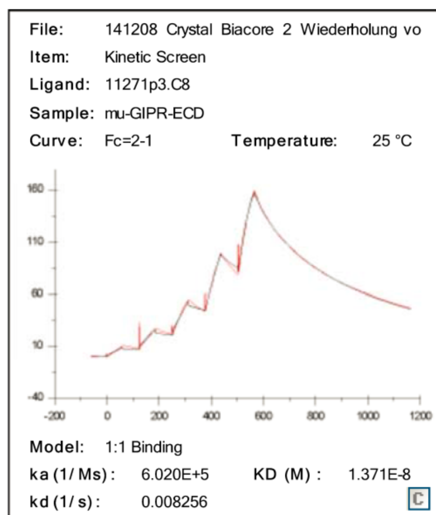

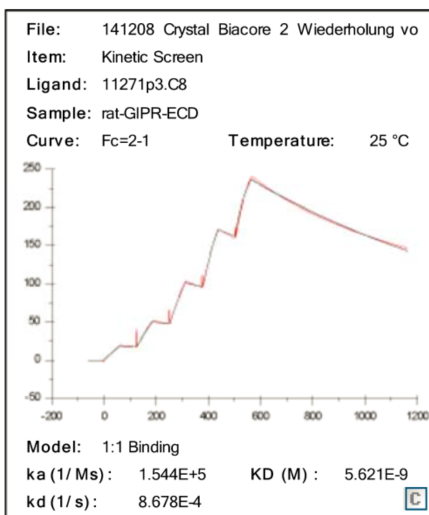

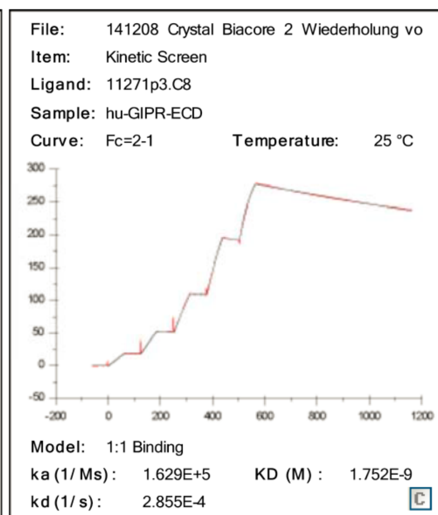

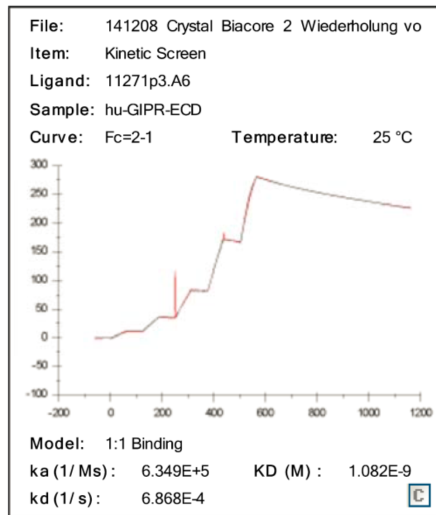

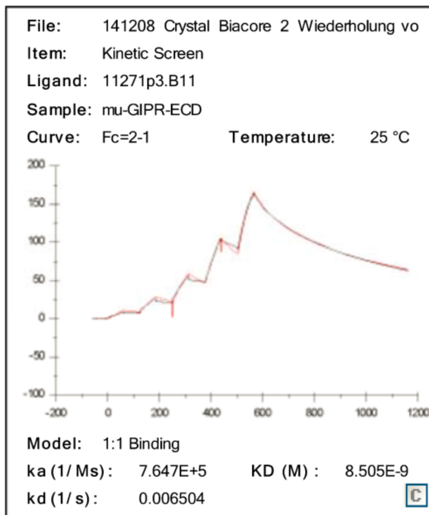

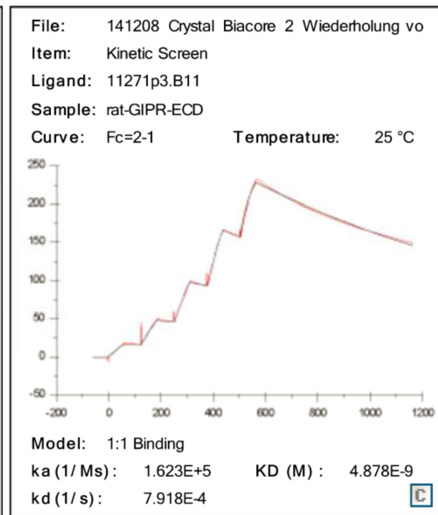

Supplement 2: Biacore Single Cylce Kinetics Data
Shown are exemplary Biacore derived Single Cycle Kinetics binding curves for three represenative antibodies (top: 11271p3.D12, middle 11271p3.C8, bottom 11271p3.A6) and human, mouse or rat derived GIPR-ECD. 5 concentrations were tested for each antibody. KD values were calculated by fitting a 1:1 binding model.

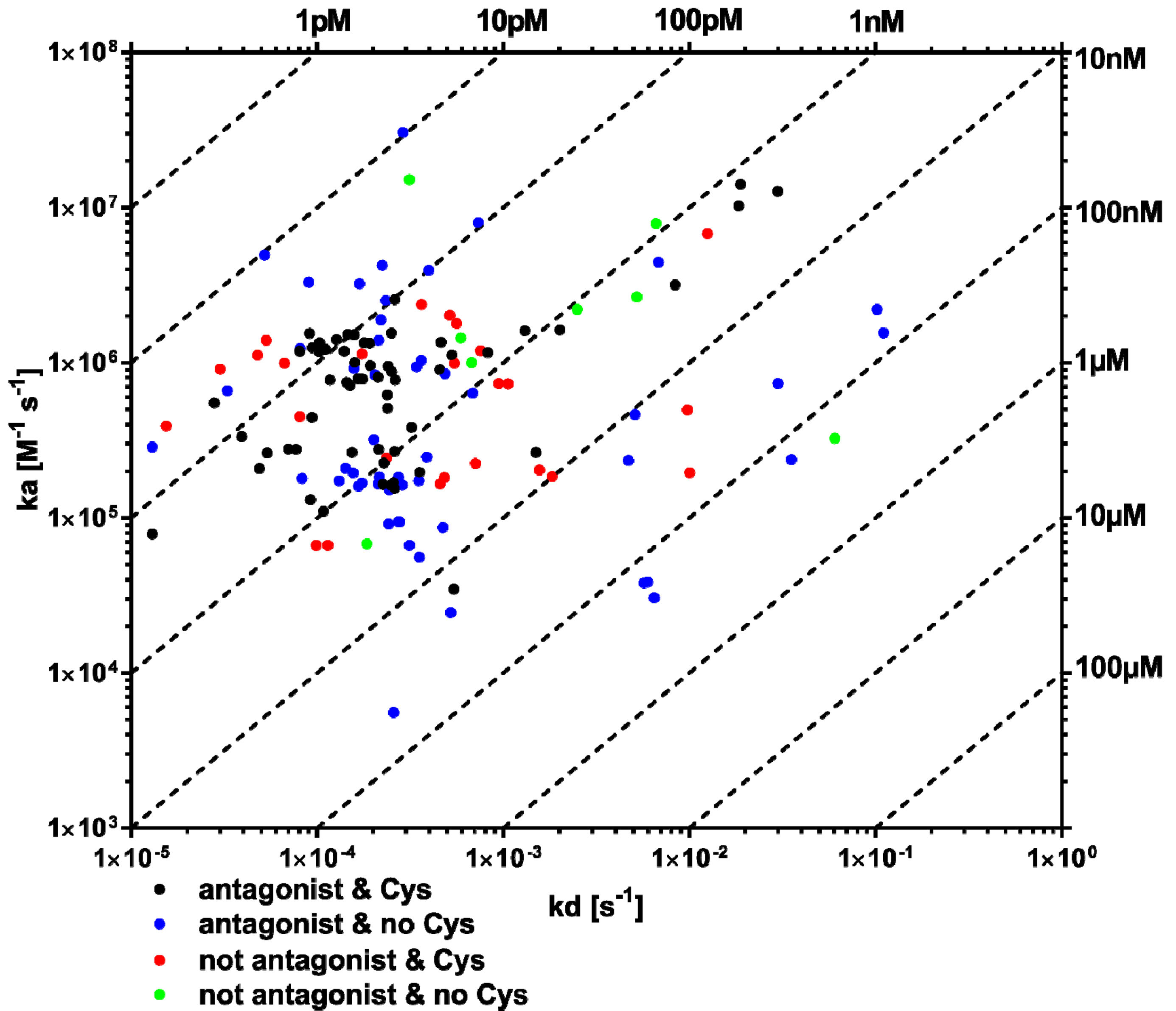

Supplement 2: Isoaffinity plot for Biacore rate constants

Shown are the on-rate (ka) and off-rate (kd) constants derived from measuring the binding of all chicken derived antibodies against the human GIPR-ECD. The diagonals indicate the KD values and the antibody populations are color coded by their ability to antagonize GIPR signaling and cysteine content.

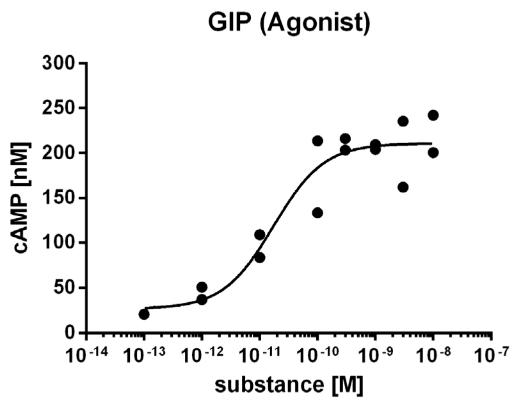

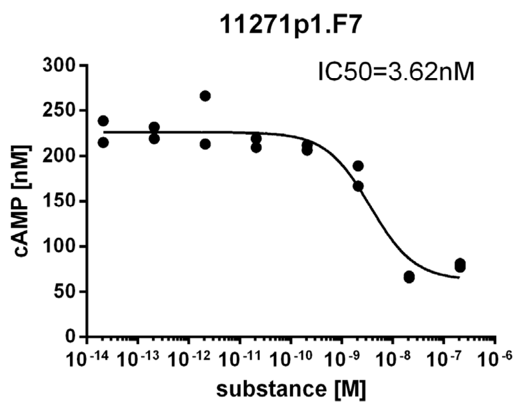

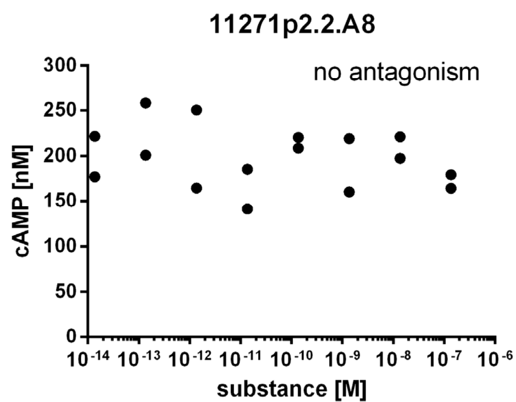

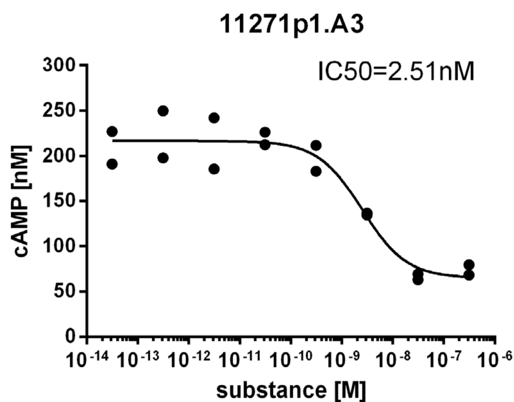

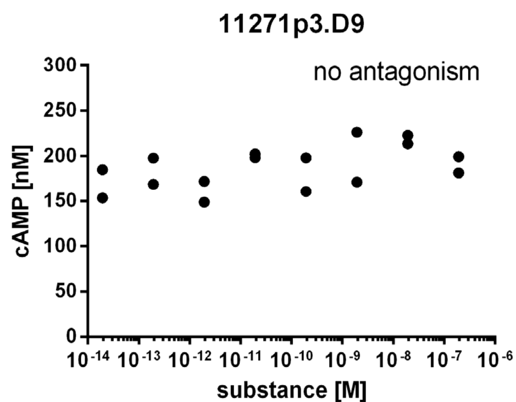

Supplement 4: Alphascreen cAMP functional assay data

Shown are representative activity data from the Alphascreen cAMP assay. The natural agonist of the GIPR GIP (top row, left) was used a positive control. As expected, it increases the cAMP signal in a concentration dependent manner. Antagonistic antibodies are able to reduce the cAMP production stimulated by GIP (11271p1.F1, 11271p1.A3), whereas non-antagonists (11271p2.2.A8, 11271p3.D9) have no impact on the amount of cAMP.

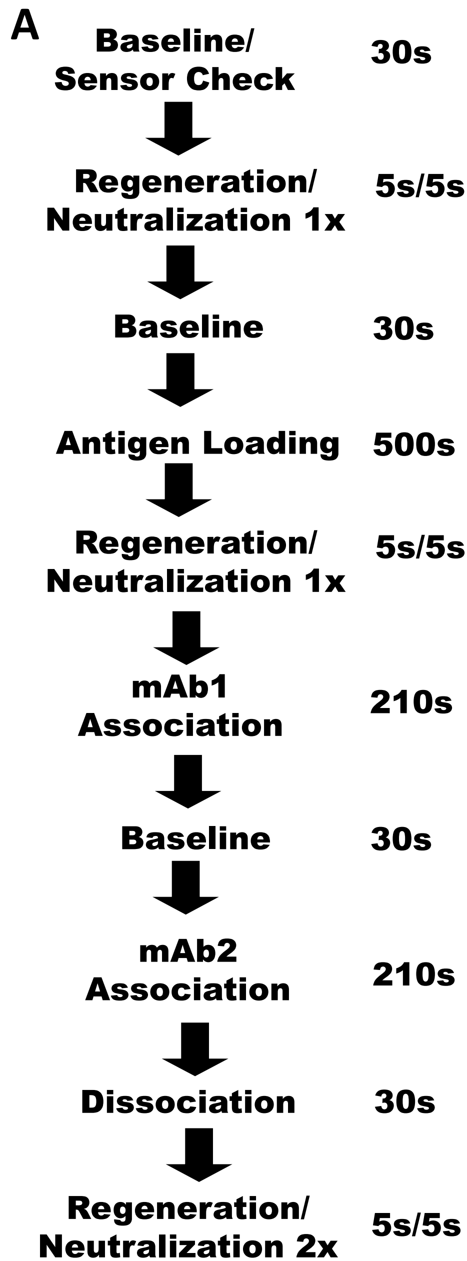

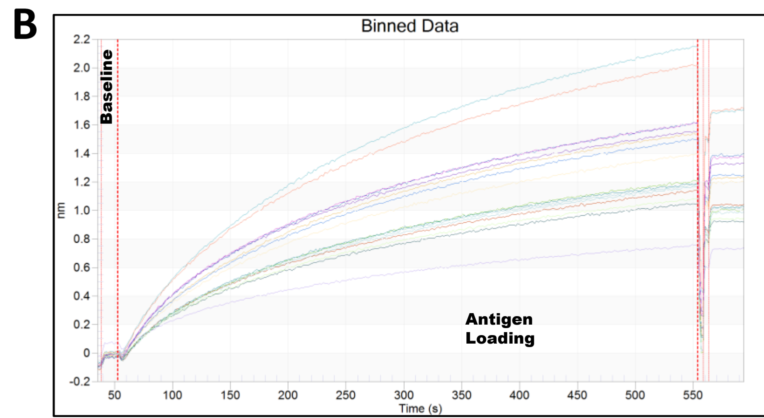

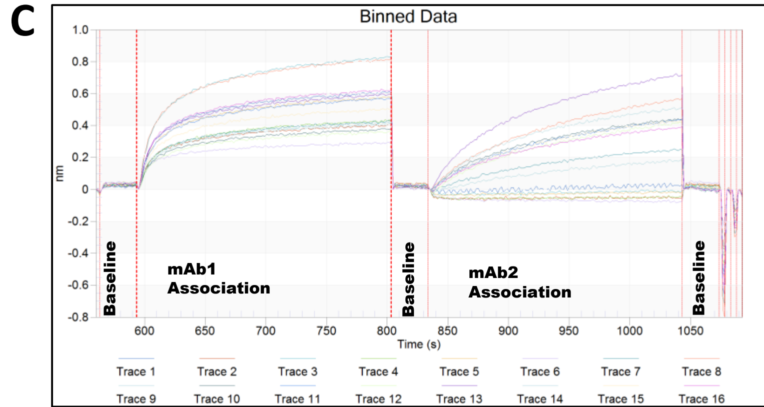

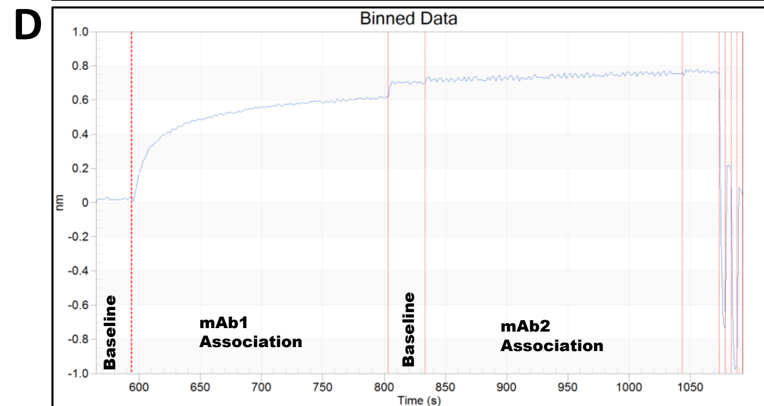

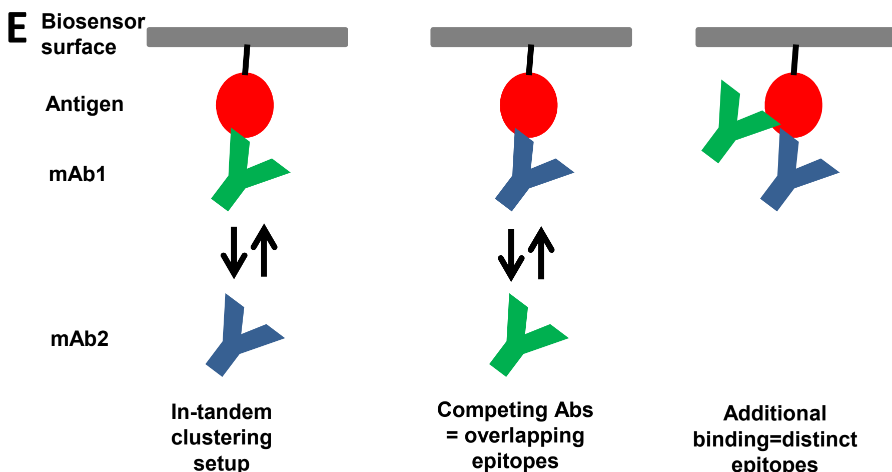

Supplement 5: Epitope Clustering by BLI

In A, the measurement step and cycling times used for BLI clustering on the Fortebio Octet HTX are shown. Antigen and test antibodies were diluted in PBS. Baseline, dissociation and neutralization steps were also performed in PBS. For Regeneration, 10mM Glycine pH 3 was used. B shows exemplary antigen immobilization data for 8 biosensors. Biotinylated human GIPR-ECD-rbFc antigen was loaded onto streptavidin biosensors. The step is sandwiched between two baselines and followed by one regeneration cycle before Ab1 and Ab2 binding are performed. In C, example data for the immobilization of Ab1 versus 16 different Ab2 is illustrated. D shows the self-binding of the pimary antibody – no additional binding occurs highlighting that the sensor surface is saturated. The absence of self-binding is essential in obtaining clean epitope clustering data. In C and D, all steps are aligned to the baseline. E gives an overview of the in-tandem epitope clustering setup. An immobilized antigen is saturated with a primary antibody and then incubated with a secondary antibody. If the secondary Ab competes with the first, no additional binding (=nm shift) occurs. An addition binding signal indicates the secondary Ab recognizing a distinct epitope.